American Mineralogist, Volume 92, pages 397–402, 2007

Organic anions in layered double hydroxides: An experimental investigation of citrate hydrotalcite

QIANG LI* AND R. JAMES KIRKPATRICK

Department of Geology, University of Illinois at Urbana-Champaign Urbana, Illinois, 61801, U.S.A.

ABSTRACT

The nature of the chemical interactions between organic species and mineral surfaces and interlayers has significant implications for many geochemical processes and for medical and materials applications, but the molecular-scale characteristics of such interactions are poorly understood. Here we describe an experimental investigation of citrate-hydrotalcite (HT) that is designed to investigate the structural environments and dynamical behavior of carboxylic species interacting with the protonated surfaces of positively charged materials such as layered double hydroxides (LDHs). X-ray diffraction, compositional analysis, and thermal analysis confirm successful intercalation of trivalent citrate anions into the interlayers of the Mg/Al hydrotalcite using an ion-exchange method. The basal spacing changes from 8.9 Å at relative humidity (R.H.) = 0% to 11.3 Å at R.H. = 75%, to 18.9 Å at 100% R.H., consistent with reorientation of the citrate from parallel to the hydroxide layers at low water contents to perpendicular to them at higher water contents. At the largest water contents, the citrate may lose contact with one of the hydroxide layers, in contrast to the behavior of LDHs containing small, inorganic species. The similarity of the ^{13}C nuclear magnetic resonance (NMR) chemical shifts for citrate-HT and sodium citrate solution demonstrates the absence of grafting (covalent bond formation) between the citrate molecules and the metal hydroxide layers, and the dominance of Coulombic and H-bond interactions in stabilizing the structure. Decreasing ^{13}C NMR peak widths, decreasing signal/noise ratios in the ^{1}H-^{13}C CPMAS NMR spectra, and increasing basal spacing with increasing R.H. are consistent with increasing dynamical disorder of the interlayer citrate sites in a progressively more water-rich interlayer.

Keywords: Citrate- HT, ion-exchange, XRD, thermal analysis, ^{1}H-^{13}C CPMAS NMR

INTRODUCTION

The interaction of solute species with mineral surfaces and in confined aqueous environments such as clay interlayers has been the subject of intense investigation for many years (Macewan and Wilson 1984; Hochella and White 1990; Valli et al. 1995; Alsaaran and Olyphant 1998; Brown et al. 1999; Savenko 2001), but focus has been principally on inorganic species (Miyata 1975; Ookubo et al. 1994; Badreddine et al. 1999; Xu and Zeng. 2001; Hou and Kirkpatrick 2002; Hou et al. 2003). With the exception of organic cations in clay interlayers, which have been studied for many years (e.g., Hoffmann and Brindley 1960; Hang and Brindley 1970; Yariv and Cross 2002), much less is known about the interaction of organic species with minerals, especially at the molecular scale. Many organic species, such as carboxylic acids, amino acids, peptides, proteins, and natural organic matter (NOM), occur as anions at most natural pH conditions, and are thus expected to interact with positively charged sites. Layered double hydroxides (LDHs) are among the few groups of minerals with permanent, positive structural charges, and they are known to intercalate and adsorb organic- and bio-molecules. Due to their large anion ion-exchange capacities (Houri et al. 1998; Badreddine et al. 1999), they offer an opportunity to investigate in detail the structural environments and molecular-scale dynamics of organic anions at mineral surfaces and in nano-confinement.

LDHs are an important class of clay-like minerals with structures based on metal hydroxide layers (Cavani et al. 1991; Ookubo et al. 1994). Replacement of a fraction of the octahedrally coordinated, divalent cations by trivalent cations results in positive layer charge that is compensated by surface and interlayer anions and associated hydrogen-bonded water molecules. Most LDHs have the general structural formula $[M^{2+}_{1-x}M^{3+}_{x}(OH)_2]^{x+}(A^{n-})_{x/n}\cdot mH_2O$, where M^{2+} (commonly Mg, Fe, Co, Cu, Ni, or Zn) and M^{3+} (commonly Al, Cr, Ga, Mn, or Fe) are di- and trivalent cations, respectively, x is the molar $M^{2+}/(M^{2+} + M^{3+})$ ratio and is in the range of 0.2–0.33, and A^{n-} is the interlayer anions.

There is a growing body of evidence that the interaction of many organic species with LDHs is weaker than that of small inorganic anions, potentially facilitating their use as, for instance, carriers of drug molecules. For LDHs containing a wide variety of inorganic anions, Hou et al. (2003) have shown that many compounds, such as Mg_3Al-CO_3 LDH, do not incorporate interlayer water and swell at any relative humidity at atmospheric pressure and that even those that do, such as Mg_3Al-SO_4 LDH, do not swell more than about 3.0 Å. In contrast, Leroux et al. (2001) have observed delamination of the hydroxide layers of Zn/Al LDH containing the surfactant dodecylsulfate by refluxing in alcohol. Hibino and Jones (2001) and Hibino and Kobayashi (2005) also reported similar exfoliation of glycine-Mg/Al LDH in formamide and lactate-containing LDHs in water. These observations suggest that the expansion behavior and thus the structural environments, dynamical behavior, and energetics

* E-mail: qiangli1@uiuc.edu

0003-004X/07/0203–397$05.00/DOI: 10.2138/am.2007.2168

of interlayer and surface species of LDH phases containing organic molecules may be significantly different than for those with inorganic anions. Little is known about the molecular scale origin of these differences.

Here we describe an experimental ^{13}C NMR, thermogravimetric, and X-ray diffraction (XRD) study of the interaction of citrate with the Mg,Al (3:1) LDH, hydrotalcite (HT). The results show that citrate-LDH exhibits greater interlayer swelling due to water incorporation than LDHs with small inorganic anions. These experimental observations in conjunction with the results of recent molecular-dynamics (MD) simulations of citrate HT (Kumar et al. 2006) suggest that there are parallel changes in molecular orientation and increasing dynamical disorder of the interlayer citrate in progressively more water-rich interlayers. The results are also in good agreement with recent experimental results for HT intercalated with glutamate, an amino acid of about the same size as citrate (Reinholdt and Kirkpatrick 2006). Citric acid is a common, naturally occurring carboxylic acid with carboxyl and hydroxyl functional groups. Organic acids, such as citrate, are known to affect nutrient acquisition and metal detoxification by plant roots, to accelerate the mobilization of some elements, such as P, Mn, and Fe, in soils (Jones 1998), and to enhance the dissolution rates of basalt and granite (Hausrath et al. 2005). Citrate also influences the stability and formation of clay-Al hydroxide polymer systems due to formation of strong complexes (Janssen et al. 1997), and recent work has shown that citrate can be readily incorporated into calcite on the molecular scale (Phillips et al. 2005). The pKas of the three –COOH groups of citric acid are 3.13, 4.76, and 6.40, and they are essentially fully deprotonated at the pH of 11.5 used for the ion exchange in this study. The CIT^{-3} anion is the stable species in this study, and the $–COO^-$ groups are thus the principal sites of interaction with the positive charge of the LDH layers and also for acceptance of H-bonds from water molecules and LDH M-OH sites. In acid solutions, citrate exhibits a more-complex, pH-dependent behavior, in which the carboxylic groups are not fully deprotonated and are thus potential sites for H-bond donation as well as acceptance (Glusker 1980).

Materials and methods

Sample preparation

The citrate-HT samples were synthesized by ion exchange for NO_3^- in NO_3-HT samples that were prepared using the co-precipitation method (Miyata 1975). 125 mL of a mixed $Mg(NO_3)_2{\cdot}6H_2O$ and $Al(NO_3)_3{\cdot}9H_2O$ solution with Mg/Al = 3 and concentrations of 2 *M* $Mg(NO_3)_2{\cdot}6H_2O$ and 0.66 *M* $Al(NO_3)_3{\cdot}9H_2O$ was added drop-wise at 55 °C into 100 mL of boiled deionized water, for which the pH was adjusted and maintained to 10 with 2 *M* NaOH solution during the addition. After delivery of the mixed nitrate solution was complete, the reaction mixture was stirred vigorously for 2 h at 55 °C under a nitrogen flow to minimize CO_2 contamination. The precipitate was then separated by centrifuging, and the product was thoroughly washed with boiled deionized water and dried under vacuum at room temperature for 6 days. To make the citrate compound, about 2 g NO_3-HT was dispersed in 100 mL of a 0.1 *M* Na-citrate solution in deionized water in a boiling flask topped by a condenser, and the mixture was allowed to react for 4 days at 65 °C under a strong nitrogen flow (Meyn et al. 1990). The resulting solution was centrifuged and the precipitate was washed 6 times with deionized water and then dried at 65 °C in a vacuum oven for 24 h. The final product was analyzed for its bulk-chemical composition and thermal behavior (TGA/DSC), and was examined by powder XRD and ^1H-^{13}C CP-MAS NMR. Aliquots of the citrate-HT were equilibrated at relative humidities (R.H.s) from near 0 to near 100% to investigate their swelling and interlayer behavior via XRD and ^{13}C NMR. The samples were maintained in separate desiccators over P_2O_5 (0% R.H.), saturated $MgCl_2{\cdot}6H_2O$ solution (33% R.H.), saturated NaCl solution (75% R.H.), and DI water (100% R.H.) (David 1998). To avoid the influence of ambient atmosphere during sample analysis, the samples were introduced into the XRD and TGA/DSC sample chambers or sealed in NMR rotors immediately after removal from the desiccators.

Experimental methods

Powder XRD patterns of unoriented samples were recorded with a Rigaku rotaflex diffractometer under the following conditions: 40 kV, 40 mA, Cu*K*α radiation (λ = 1.5406 Å). The sample was scanned in steps of 0.02 °2θ in the range from 3 to 70° using a counting time of 3 s per step under ambient conditions, and basal spacings were determined from the position of the *d*(003) reflection. Low-angle XRD data were obtained from 0.76 to 59.96 °2θ for citrate-HT equilibrated at 100% R.H. using a Philips X'pert diffractometer with Cu*K*α radiation a step size of 0.08 °2θ and a counting time of 3 s/step. Simultaneous thermogravimetric analysis (TGA) and differential scanning calorimetry (DSC) curves were obtained with a Netzsch STA 409 Thermal Analyzer. About 60 mg of sample were heated from room temperature to 1300 °C at a heating rate of 5 °C/min under flowing air. For compositional analysis, Al and Mg were determined using an Inductively Coupled Plasma (ICP) emission spectrometer. Carbon, H, and N were determined with a model CE440 CHN analyzer from Exeter Analytical Inc.

For the as-synthesized citrate-HT samples, the ^1H-^{13}C cross polarization (CP) MAS NMR spectra were obtained at room temperature using a General Electric GN300WB spectrometer (H_0 = 7.05 T) and a 7 mm Chemagnetics MAS probe. The 90° pulse durations and relaxation delays were 6.5 µs and 1.25 s, respectively; the contact time was 4000 µs, the MAS frequency was ~6 kHz, 5000 transients were collected, and the chemical shifts are referenced to the methyl group of external hexamethyl benzene (HMB) at 17.3 ppm. For the samples equilibrated at different R.H.s, the ^1H-^{13}C experiments were performed using a 4 mm probe at a MAS frequency of ~9 kHz, a contact time of 2000 µs, a relaxation delay of 1.25 s, and a 90° pulse of 3 µs. 2048 transients were recorded, and the chemical shifts are referenced to the methyl group of external glycine at 43.6 ppm. The ^{13}C spectrum of 1M sodium citrate solution was colleted using a Varian VXB500 spectrometer and a 10 mm broadband solution probe. The 90° pulse durations and the relaxation delays for this experiment were 6 µs and 5 s, respectively. After their acquisition, the free induction decays (FID) were treated following standard procedures using the NMR Utility Transform Software (NUTS, Acorn NMR software).

Results and discussion

Chemical composition

The analyzed composition of the as-synthesized citrate-HT sample (average of two analyses in wt%) is Mg, 19.98%; Al, 7.49%; C, 6.38%; H, 4.03%; N, 0.14%. The structural formula for the room R.H. citrate-HT obtained from these data and the water content from TGA (see below) is $(Mg_{3.01},Al)(OH)_8(C_6H_5O_7)^{3-}_{0.32}(NO_3)_{0.04}(CO_3)^{2-}_{0.01}{\cdot}3.9H_2O$. This is based on an 8 (OH) formula, and the 1σ accuracy based on replicate analyses of Mg and Al is about 0.3%. The structural formula also assumes that citrate occurs as the CIT^{3} anion ($C_6H_5O_7^{-3}$), which is consistent with the relatively acid pKas of its –COOH groups and the pH = 11.5 of the final ion-exchange solution. The molar Mg/Al ratio of essentially 3 indicates that the co-precipitation reaction was complete. The analyses also show a small amount of residual nitrate due to incomplete ion exchange as well as a small amount of CO_3^{2-}, which has a strong affinity for LDHs (Miyata 1983). The water content was calculated from the TGA data, which shows 19% weight loss at low temperature (see thermal analysis results below), all of which is attributed to interlayer water in the structural formula.

XRD

The XRD pattern of the as-synthesized, room humidity NO_3^--HT precursor shows the characteristic peaks of well-crystallized hydrotalcite with a basal spacing of 8.0 Å (Fig. 1A), in agreement with previously published values (Hou et al. 2000). After

citrate for NO_3^- exchange, the (003) basal spacing increases to 11.7 Å (Fig. 1B), clearly showing citrate intercalation and consistent with the chemical analysis. The 8.0 Å basal spacing for NO_3^-HT has been previously shown to be due to the NO_3^- being orientated parallel to the HT layers (Arco et al. 2000). The citrate molecule is ~7.0 Å long and adding this to the ca. 4.8 Å thickness of the Mg,Al (3:1) hydroxide layer, indicates that the 11.7 Å basal spacing is due to interlayer citrate being oriented almost perpendicular to the hydroxide layers in the as-synthesized state at room conditions. MD simulations of citrate-HT are consistent with this conclusion (Kumar et al. 2006).

The basal spacing of the citrate-HT changes significantly with varying R.H. (Fig. 2). At 0% RH, the (003) basal peak is relatively broad with a maximum at 8.9 Å (9.9 °2θ) for citrate-HT and a shoulder from residual NO_3^--HT and contaminating CO_3^{2-}-HT at 7.8 Å. With increasing R.H., the basal spacing of the citrate phase increases from 8.9 to 10.9 Å at 33% R.H., and to 11.3 Å at 75% R.H. (essentially the same as for the as-synthesized sample). The (003) peak for citrate-HT also becomes narrower with increasing R.H., indicating a decreased distribution of interlayer spacings in this R.H. range. At 100% R.H., the XRD pattern obtained with the Philips X'pert diffractometer shows a broad tail at <5 °2θ, but that from the Philips instrument, which is optimized for lower angle diffraction shows a basal (003) peak of ~18.9 Å (~4.7 °2θ). The poorly resolved intensity near ~9.5 °2θ is assigned to the (006) of the citrate phase, and the relatively broad peak at ~11.5 °2θ to the nitrate and carbonate phases, which do not swell significantly with increasing R.H. (Hou et al. 2003).

The increased basal spacing of citrate-HT from 8.9 Å at 0% R.H. to 11.3 Å at 75% R.H. indicates a change in orientation of the CIT^{-3} ions from parallel to the metal hydroxide layers to a high angle to them with increasing hydration. The expansion to ~19 Å at 100% R.H. requires that the citrate molecules lose contact with at least one side of the interlayer. The MD simulations of Kumar et al. (2006) are fully consistent with these conclusions. With no interlayer water, the models show the CIT^{-3} lying parallel to the interlayer due to Coulombic attraction and H-bonding between the M-OH groups and the $-COO^-$. At moderate hydration levels, the simulations show the CIT^{-3} to be in contact with both sides of the interlayer but oriented essentially perpendicular to it. This orientation lowers the overall energy by allowing the CIT^{-3} to accept a larger fraction of their H-bonds from water resulting in a well-integrated H-bond network among them, the H_2O, and the M-OH sites. At high water contents, the MD simulations show that CIT^{-3} occurs dominantly as outer-sphere complexes associated with only one side of the interlayer, and that the molecular orientation is dynamically disordered. This conclusion is also consistent with results for Mg_2Al HT containing the amino acid glutamate, which exhibits similar behavior at 100% R.H. (Reinholdt and Kirkpatrick 2006). Glutamate is similar in size to citrate and occurs as the GLU^{-1} and GLU^{-2} anions. Together with the observed delamination of Gly-LDH and Lact-LDH (Hibino and Jones 2001; Hibino and Kobayashi 2005), these observations confirm the suggestion that moderate-size organic molecules interact less strongly with the hydroxide layers of LDHs than smaller, inorganic species such as NO_3^- and Cl^- (Wang et al. 2001; Hou et al. 2003). Hou et al. (2003) used variable R.H. XRD and thermal analysis data for Mg_3Al and $LiAl_2$ LDH phases containing various inorganic anions to show that these phases behave in three different ways in terms of water sorption and the associated effects on the structural environments and dynamics of the interlayer anions. One group of phases is characterized by 1.5–3.0 Å expansion to a two-water layer structure (e.g., Mg_3Al-SO_4). The second type is slightly expandable (<0.5 Å) and forms only one-water layer structures (e.g., $LiAl_2$-Cl). The third type is essentially non-expandable (0~0.2 Å) and exhibits little interlayer water exchange (e.g., Mg_3Al-CO_3). The results

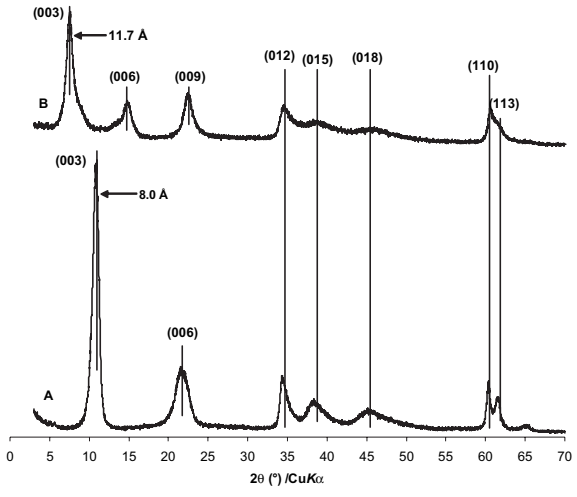

FIGURE 1. XRD patterns of nitrate hydrotalcite (A) and citrate hydrotalcite (B).

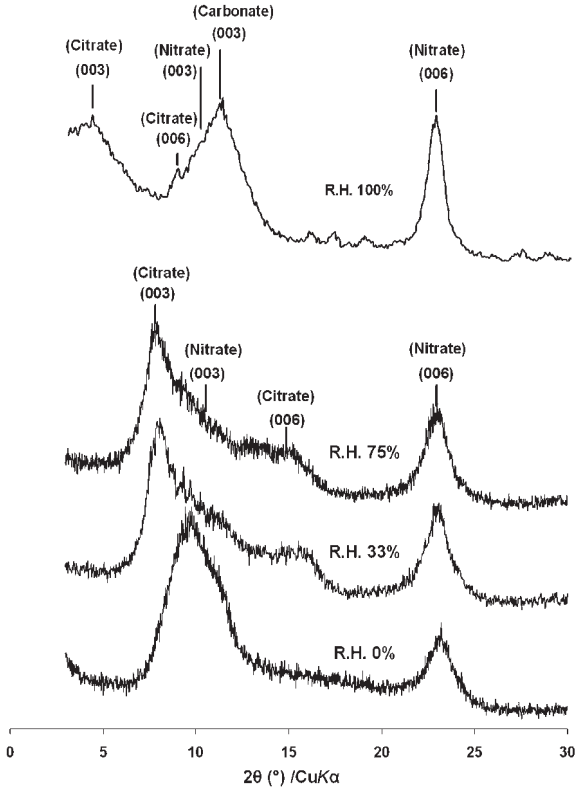

FIGURE 2. XRD patterns citrate hydrotalcite at the indicated R.H.s.

for citrate-, glutamate-HT (Reinholdt and Kirkpatrick 2006), Gly-LDH (Hibino et al. 2001), Lact-LDH (Hibino and Kobayashi 2005), and dodecylsulfate LDH (Leroux et al. 2001) suggest that LDHs containing moderately sized organic anions exhibit a fourth type of behavior in which the anions are relatively weakly bound to the hydroxide layers allowing significantly greater expansion. This behavior may be related to a combination of (1) a lower charge density on the organic species, (2) a somewhat smaller charge on the O atoms of the $–COO^-$ groups than on the O atoms of water, and (3) the need to develop a an integrated H-bond network among the M-OH groups, the anions, and the water molecules.The MD modeling results for citrate-HT show a large thermodynamic driving force for water incorporation into the interlayer at high water contents.

Thermal analysis

The TGA/DSC patterns for NO_3^-- and citrate-HT show many similarities but also significant differences due to the citrate for nitrate exchange (Fig. 3). NO_3^--HT shows a well-resolved weight loss of about 14% between 60 and 200 °C followed by a series of four less-well-resolved weight losses totaling about 35% between 320 and 750 °C (Fig. 3A). The corresponding DSC pattern shows large endotherms at 125 and 385 °C with poorly resolved shoulders at higher temperatures of each, and three smaller endotherms near 495, 550, and 680 °C. All of these endotherms are centered at one of the weight loss features. As is usual for layered double hydroxides (Miyata 1975; Zhang et al. 2004; Arco et al. 2000), the weight loss and corresponding endotherm near 125 °C are readily assigned to loss of interlayer and surface water molecules (dehydration), and the features near 385 °C to simultaneous partial dehydroxylation of the hydroxide layers and nitrate decomposition. The feature near 495 °C is probably related to decomposition of carbonate (Stanimirova et al. 2004), and the small endothermic features near 550 and near 700 °C probably arise from loss of the most strongly held OH-groups.

The as-synthesized citrate-HT sample shows three weight-loss features totaling about 19% between room temperature and 235 °C and a second weight loss of about 30% beginning at ~330 °C and ending at 480 °C (Fig. 3B). The DSC pattern shows three resolved endotherms centered at 115, 175, and 225 °C in the range of the low temperature weight loss. Between about 300 and 500°C, there are a series of overlapping endothermic and exothermic peaks in the same temperature range as the major weight loss centered near 400 °C. As for the nitrate phase (and other LDHs described in the literature), the features below 235 °C are due to loss of surface and interlayer water molecules. The endothermic peak at 225 °C, which is not present for the nitrate-HT, may be due to decarboxylation of citrate molecules (Rajendran and Rao 1994). The higher-temperature features between 300 and 500 °C are readily assigned to simultaneous dehydroxylation (endothermic), citrate combustion (exothermic), and decomposition of nitrate and carbonate (endothermic) (Constantino and Pinnavaia 1995; Arco et al. 2000).

It has been previously proposed that intercalation of organic- and bio-molecules in LDH interlayers protects them from thermal decomposition to higher temperatures than in the native state (Darder et al. 2005), and our results for citrate-HT are consistent with that conclusion. The DSC pattern for trisodium citrate dihydrate ($Na_3C_6H_8O_7 \cdot 2H_2O$) (Fig. 3C) shows one well-resolved endothermic feature at 170 °C due to melting and water loss, and four exothermic peaks at 240, 302, 350, and 425 °C due to progressive, multiple-step combustion of the citrate molecules accompanied by intra-molecular dehydroxylation and decarboxylation (Rajendran and Rao 1994). The main citrate decomposition takes place between 230 and 450°C. This is about 100° lower than for citrate-HT, consistent with a protective effect

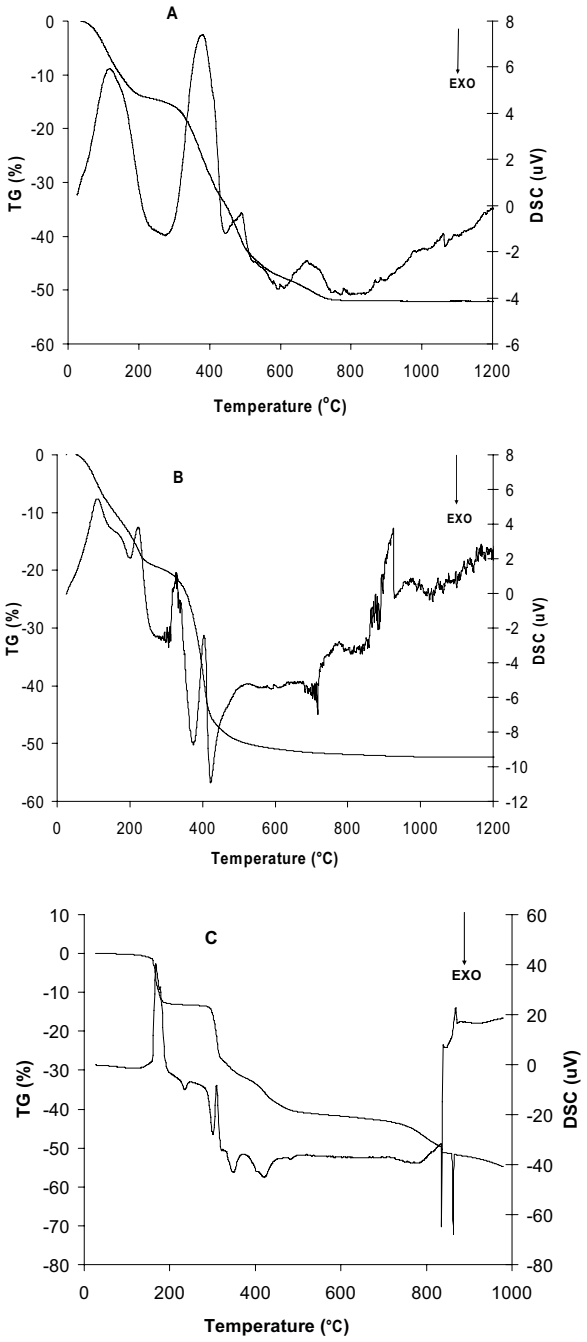

FIGURE 3. TGA/DSC patterns of nitrate hydrotalcite (**A**), citrate hydrotalcite (**B**), and crystalline trisodium citrate dihydrate (**C**).

of the Mg,Al hydroxide layers of hydrotalcite that increases the thermal stability of the CIT^{-3}.

^{13}C NMR Spectroscopy

The ^{13}C CP-MAS NMR spectra of the as-synthesized citrate-HT and the citrate-HT samples equilibrated at different R.H.s all exhibit relatively broad peaks at about 181.7, 179.6, 75.7, and 46.1 ppm that can be readily assigned to the central $–COO^–$, terminal $–COO^–$, -COH, and $–CH_2$ groups, respectively (Fig. 4A) (Fischer et al. 1995). The ^{13}C NMR spectrum of 1 *M* Na-citrate solution shows much narrower resonances at essentially the same chemical shifts (Fig. 4B). NMR chemical shifts are very sensitive to local chemical environments, and especially to changes in the extent of covalent bonding (Profeta et al. 2004). Thus, the lack of change in the chemical shifts due to intercalation clearly demonstrates that intercalation of citrate does not result in its grafting to the hydroxide layers [formation of covalent linkages such as C-O-(Mg, Al)]. Citrate molecules, then, interact with the LDH hydroxide layers primarily through Coulombic attraction and H-bonding, as previously observed for inorganic anions (Hou et al. 2000, 2002; Khan and O'Hare 2002) and glutamate (Aisawa et al. 2001; Reinholdt and Kirkpatrick 2006). The small peak at near 170.0 ppm for the citrate-HT is due to carbonate, as observed in the compositional analysis.

The large widths of the peaks for citrate in HT (4–10 ppm full width at half maximum) suggest that the intercalated and surface citrate molecules occur with different structural confirmations, although these cannot be explicitly identified from the NMR results.

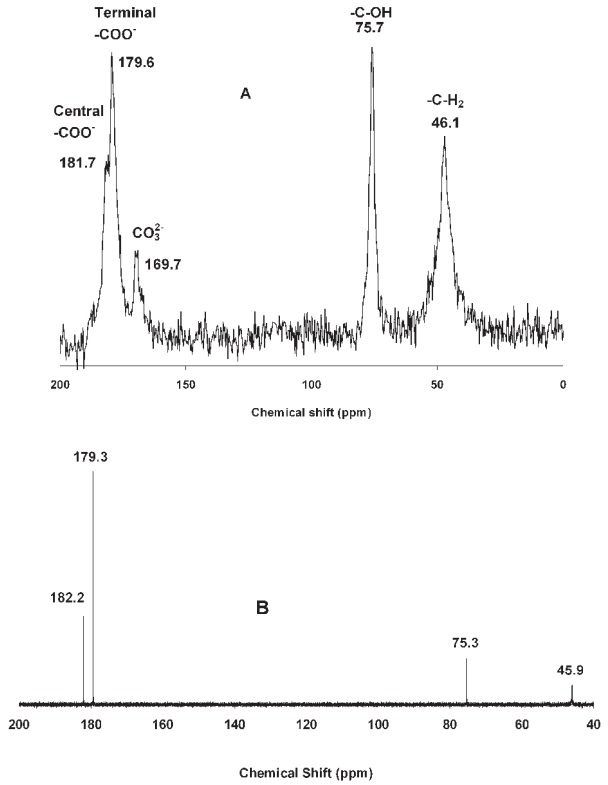

FIGURE 4. ^{13}C CP-MAS NMR spectra of citrate hydrotalcite (**A**) and ^{13}C NMR spectrum of 1 *M* sodium citrate solution (**B**).

Citrate salts are known to contain three different citrate conformations (Glusker 1980). One of these has the citrate backbone fully extended in a planar zigzag pattern. The other two have one of the terminal carbon atoms swung around with the dihedral angle formed by the terminal carbon, central carbon, and two adjacent CH_2 groups approximately equal to +60° or –60°. These two are related by mirror symmetry. The MD modeling of citrate hydroltalcite identifies similar conformations, which are referred to as boat-boat, boat-chair, and chair-boat (Kumar et al. 2006). It is likely that the presence of these three conformations as well as strain of the molecules due to interlayer confinement contribute to the observed peak widths.

With increasing R.H., the ^{13}C CP MAS NMR spectra of citrate-HT show progressively narrower peak widths, increasing resolution of all peaks, and decreasing signal/noise ratios, but there are no significant changes in the chemical shifts (Fig. 5). The observed peak narrowing and decreased signal/noise ratios are most likely due to dynamical effects caused by increasing interlayer hydration with increasing R.H. CP signal intensity at a given contact time depends on the magnitude of the ^{1}H-^{13}C dipolar coupling (Alemany et al. 1983), which is related to the number of nearby H-spins, their distances from the observed nuclei, and the extent of dynamical self-decoupling due to relative ^{1}H and ^{13}C dipolar reorientation. At 0% R.H., the relatively large signal noise ratio may be due to the citrate being rigidly held in the interlayer, as also shown by the MD simulations (Kumar et al. 2006). Under these conditions, the CP intensity arises from the ^{1}H values of the citrate –COH and $–CH_2$ groups and from the protons of the metal hydroxide layers. The poor resolution is due

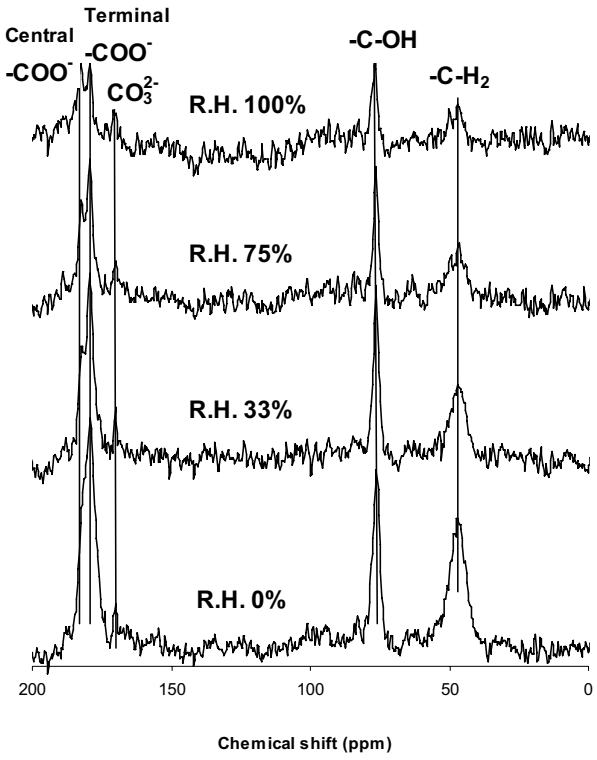

FIGURE 5. ^{13}C CP-MAS NMR spectra of citrate hydrotalcite equilibrated at the indicated R.H.s.

to a range of local –COO^- environments, perhaps with a range of C-C bond angles due to different conformations and molecular strain (Oldfield 2005). With increasing R.H., the more solution-like environment of the expanded interlayer allows increased citrate reorientational motion. Such dynamics are observed in the MD simulations. This motion reduces the dipolar broadening, resulting in narrower peaks and decreased CP intensity. These dynamical effects, however, do not become as effective as in bulk solution, as illustrated by the narrower peak widths for the Na-citrate solution (Fig. 4B). A similar decrease of ^1H-^{13}C CP intensity with increasing R.H. occurs for glutamate-HT (Reinholdt and Kirkpatrick 2006), for which the results suggest nearly complete loss of CP signal for molecules located on external surfaces.

ACKNOWLEDGMENTS

This paper was supported by grant DOEFG02-00ER15028 from the Geoscience program of the U.S. Department of Energy Division of Basic Energy Sciences. The authors would like to thank Marc Reinholdt, Xiaoqiang Hou, Padma P. Kumar, and P.K. Babu for their useful discussion on the experiments. Some of the XRD experiments were carried out in the Center for Microanalysis of Materials, University of Illinois, which is partially supported by the U.S. Department of Energy under grant DEFG02-91-ER45439.

REFERENCES CITED

Aisawa, S., Takahashi, S., Ogasawara, W., Umetsu, Y., and Narita, E. (2001) Direct intercalation of amino acids into layered double hydroxides by coprecipitation. Journal of Solid State Chemistry, 162, 52–62.

Alemany, L.B., Grant, D.M., Pugmire, R.J., Alger, T.D., and Ailm, K.W. (1983) Cross polarization and magic angle sample spinning NMR spectra of model organic compounds. 1. highly protonated molecules. Journal of American Chemical Society, 105, 2133–2141.

Alsaaran, N. and Olyphant, G.A. (1998) A model for simulating rock-water interactions in a weathering profile subjected to frequent alternations of wetting and drying. Catena, 32, 225–243.

Arco, D.M., Gutierrez, S., Martin, C., Rives, V., and Rocha J. (2000) Effect of the Mg: Al ratio on borate (or silicate)/nitrate exchange in hydrotalcite. Journal of Solid State Chemistry, 151, 272–280.

Badreddine, M., Legrouri, A., Barroug, A., Roy, A.D., and Besse, J.P. (1999) Ion exchange of different phosphate ions into the zinc-aluminium-chloride layered double hydroxide. Materials Letters, 38, 391–395.

Brown, G.E., Jr., Foster, A.L., and Ostergren, J.D. (1999) Mineral surfaces and bioavailability of heavy metals: A molecular-scale perspective, 96, p. 3388–3395. National Academy of Sciences colloquium "Geology, Mineralogy, and Human Welfare," November 8–9, 1998, Irvine, California.

Cavani, F., Trifiro, F., and Vaccari, A. (1991) Hydrotalcite-type anionic clays: Preparation, properties, and applications. Catalysis Today, 11, 173–301.

Constantino, V.R.L. and Pinnavaia, T.J. (1995) Basic properties of $Mg^{2+}_{1-x}Al^{3+}_x$ layered double hydroxides intercalated by carbonate, hydroxide, chloride, and sulfate anions. Inorganic Chemistry, 34, 883–892.

Darder, M., Lopez-Blanco, M., Aranda, P., Leroux, F., and Ruiz-Hitzky, E. (2005) Bio-nanocomposites based on layered double hydroxides. Chemistry of Materials, 17, 1969–1977.

David, R.L. (1998) CRC Handbook of Chemistry and Physics. CRC Press, Boca Raton, Florida.

Fischer, J.W., Merwin, L.H., and Nissan, R.A. (1995) NMR investigation of the thermolysis of citric acid. Applied Spectroscopy, 49, 120–126.

Glusker, J.P. (1980) Citrate conformation and chelation: enzymatic implications. Accounts of Chemical Research, 13, 345–352.

Hang, P.T. and Brindley, G.W. (1970) Methylene blue absorption by clay minerals. Determination of surface areas and cation exchange capacities (Clay-organic studies XVIII). Clays and Clay Minerals, 18, 203–212.

Hausrath, E.M., Neaman, A., and Brantley, S.L. (2005) Basalt and granite dissolution rates in the presence of citrate. Abstract for the15th Annual V.M. Goldschmidt Conference, Moscow, Idaho.

Hibino, T. and Jones, W. (2001) New approach to the delamination of layered double hydroxides. Journal of Materials Chemistry, 11, 1321–1323.

Hibino, T. and Kobayashi, M. (2005) Delamination of layered double hydroxides in water. Journal of Materials Chemistry, 15, 653–656.

Hochella, M.F. and White, A.F. (1990) Mineral–Water interface geochemistry: an overview. In M.F. Hochella and A.F. White, Eds., Mineral–Water Interface Geochemistry, 23, p. 1–16. Reviews in Mineralogy, Mineralogical Society of America, Chantilly, Virginia.

Hoffmann, R.W. and Brindley, G.W. (1960) Adsorption of non-ionic aliphatic molecules from aqueous solutions on montmorillonite. Clay Organic Studies II. Geochimica et Cosmochimica Acta, 20, 15–29.

Hou, X. and Kirkpatrick, R.J. (2002) Interlayer structure and dynamics of ClO_4^- layered double hydroxides. Chemistry of Materials, 14, 1195–1200.

Hou, X., Kirkpatrick, R.J, Yu, P., Moore D., and Kim, Y. (2000) ^{15}N NMR study of nitrate ion structure and dynamics in hydrotalcite-like compounds. American Mineralogist, 85, 173–180.

Hou, X., Kalinichev, A.G., and Kirkpatrick, R.J. (2002) Interlayer structure and dynamics of Cl^--$LiAl_2$-layered double hydroxide: ^{35}Cl NMR observations and molecular dynamics modeling. Chemistry of Materials, 14, 2078–2085.

Hou, X., Bish, D.L., Wang, S.-L., Johnston, C.T., and Kirkpatrick, R.J. (2003) Hydration, expansion, structure, and dynamics of layered double hydroxides. American Mineralogist, 88, 167–179.

Houri, B., Legrouri, A., Barroug, A., Forano, C., and Besse, J.P. (1998) Use of the ion-exchange properties of layered double hydroxides for water purification. Collection of Czechoslovak Chemical Communications, 63(5), 732–740.

Janssen, R.P.T., Bruggenwert, M.G.M., and Riemsdijk, W.H.V. (1997) Interactions between citrate and montmorillonite-Al hydroxide polymer systems. European Journal of Soil Science, 48, 463–472.

Jones, D.L. (1998) Organic acids in the rhizosphere—a critical review. Plant and Soil, 205, 25–44.

Khan, A.I. and O'Hare, D. (2002) Intercalation chemistry of layered double hydroxides: recent developments and application. Journal of Materials Chemistry, 12, 3191–3198.

Kumar, P.P., Kalinichev, A.G., and Kirkpatrick, R.J. (2006) Hydration, Swelling, Interlayer Structure and Hydrogen Bonding in Organo-Layered Double Hydroxides: Insights from Molecular Dynamics Simulation of Citrate-Intercalated Hydrotalcite. Journal of Physical Chemistry B, 110, 3841–3844.

Leroux, F., Adachi-Pagano, M., Intissar, M., Chauviere, S., Forano, C., and Besse, J.P. (2001) Delamination and restacking of layered double hydroxides. Journal of Materials Chemistry, 11, 105–112.

Macewan, D.M.C. and Wilson, M.J. (1984) Interlayer and intercalation complexes of clay minerals. In G.W. Brindley and G. Brown, Eds., Crystal structures of clay minerals and their X-ray identification, p. 197–248. Mineralogical Society, London.

Meyn, M., Beneke, K., and Lagaly, G. (1990) Anion-exchange reactions of layered double hydroxides. Inorganic Chemistry, 29, 5201–5207.

Miyata, S. (1975) The synthesis of hydrotalcite-like compounds and their structures and physico-chemical properties—I: the systems Mg^{2+}-Al^{3+}-NO_3^-, Mg^{2+}-Al^{3+}-Cl^-, Mg^{2+}-Al^{3+}-ClO_4^-, Ni^{2+}-Al^{3+}-Cl^- and Zn^{2+}-Al^{3+}-Cl^-. Clays and Clay Minerals, 23, 369–375.

——— (1983) Anion-exchange properties of hydrotalcite-like compounds. Clays and Clay Minerals, 31, 305–311.

Oldfield, E. (2005) Quantum chemical studies of protein structure. Philosophical Transactions of the Royal Society of London, Series B: Biological Sciences, 360, 1347–1361.

Ookubo, A., Ooi, K., Tani, F., and Hayashi, H. (1994) Phase transition of Cl^--intercalated hydrotalcite-like compound during ion exchange with phosphates. Langmuir, 10, 407–411.

Phillips, B.L., Lee, Y.J., and Reeder, R.J. (2005) Organic coprecipitates with calcite: NMR spectroscopic evidence. Environmental Science and Technology, 39(12), 4533–4539.

Profeta, M., Benoit, M., Mauri, F., and Pickard, C.J. (2004) First-principles calculation of the ^{17}O NMR parameters in Ca oxide and Ca aluminosilicates: the partially covalent nature of the Ca-O bond, a challenge for density functional theory. Journal of the American Chemical Society, 126, 12628–12635.

Rajendran, M. and Rao, S.M. (1994) Formation of $BaTiO_3$ from citrate precursor. Journal of Solid State Chemistry, 113, 239–247.

Reinholdt, M.X. and Kirkpatrick, R.J. (2006) Experimental Investigations of Amino Acid-Layered Double Hydroxide Complexes: Glutamate-Hydrotalcite. Chemistry of Materials, 18, 2567–2576.

Savenko, A.V. (2001) Interaction between Clay Minerals and Fluorine-Containing Solutions. Water resources, 28, 274–277.

Stanimirova, T., Piperov, N., Petrova, N., and Kirov, G. (2004) Thermal evolution of Mg-Al-CO_3 hydrotalcites. Clay Minerals, 39, 177–191.

Valli, M., Malmensten, B., and Persson, I. (1995) A vibration spectroscopic study on the interaction between some sulphide minerals and tris-(2-cyanoethyl)phosphine in aqueous solution. Colloids and Surfaces, 99, 201–205.

Wang, J., Kalinichev, A.G., Kirkpatrick, R.J., and Hou, X. (2001) Molecular modeling of the structure and energetics of hydrotalcite hydration. Chemistry of Materials, 13, 145–150.

Xu, Z.P. and Zeng, H.C. (2001) Ionic intercalations in crystallite growth of CoMgAl-hydrotalcite-like compounds. Chemistry of Materials, 13, 4555–4563.

Yariv, S. and Cross, H. (2002) Organo-Clay Complexes and Interactions. Marcel Dekker Inc., New York.

Zhang, J., Zhang, F.Z., Ren, L.L., Evans, D.G., and Duan, X. (2004) Synthesis of layered double hydroxide anionic clays intercalated by carboxylate anions. Materials Chemistry and Physics, 85, 207–214.

MANUSCRIPT RECEIVED NOVEMBER 23, 2005
MANUSCRIPT ACCEPTED OCTOBER 3, 2006
MANUSCRIPT HANDLED BY MICHAEL FECHTELKORD